



LC/MS/MS analyses of open-flow microperfusion samples quantify eicosanoids in a rat model of skin inflammation^S

Cornelia Pipper,^{*,†} Natalie Bordag,[†] Bernadette Reiter,^{*} Kyriakos Economides,[§] Peter Florian,^{**,§} Thomas Birngruber,^{*} Frank Sinner,^{*} Manfred Bodenlenz,^{*} and Anita Eberl^{1,*,§}

Joanneum Research Forschungsgesellschaft mbH,^{*} Institute for Biomedicine and Health Sciences, Graz, Austria; Center for Biomarker Research in Medicine,[†] Graz, Austria; Type 2 Inflammation and Fibrosis,[§] Immunology and Inflammation Research TA, Sanofi, Framingham, MA; and Type 1/17 Immunology and Arthritis Cluster,^{**} Immunology and Inflammation Research TA, Sanofi, Frankfurt am Main, Germany

ORCID IDs: 0000-0002-9505-6271 (N.B.)

Abstract Eicosanoids are lipid-mediator molecules with key roles in inflammatory skin diseases, such as psoriasis. Eicosanoids are released close to the source of inflammation, where they elicit local pleiotropic effects and dysregulations. Monitoring inflammatory mediators directly in skin lesions could provide new insights and therapeutic possibilities. Here, we analyzed dermal interstitial fluid samples obtained by dermal open-flow microperfusion in a rat model of skin inflammation. We developed a solid-phase extraction ultra-HPLC/MS/MS method to reliably and precisely analyze small-volume samples and quantified 11 eicosanoids [thromboxane B₂, prostaglandin (PG) E₂, PGD₂, PGF_{2α}, leukotriene B₄, 15-HETE, 12-HETE, 5-HETE, 12-hydroxyeicosapentaenoic acid, 13-HODE, and 17-hydroxydocosahexaenoic acid]. Our method achieved a median intraday precision of approximately 5% and interday precision of approximately 8%. All calibration curves showed excellent linearity between 0.01 and 50 ng/ml ($R^2 > 0.980$). In the rat model, eicosanoids were significantly increased in imiquimod-treated inflamed skin sites compared with untreated control sites. Oral treatment with an anti-inflammatory glucocorticoid decreased eicosanoid concentrations.^S These results show that a combination of tissue-specific sampling with LC/MS analytics is well suited for analyzing small sample volumes from minimally invasive sampling methods such as open-flow microperfusion or microdialysis to study local inflammation and the effect of treatments in skin diseases.—Pipper, C., N. Bordag, B. Reiter, K. Economides, P. Florian, T. Birngruber, F. Sinner, M. Bodenlenz, and A. Eberl. **LC/MS/MS analyses of open-flow**

microperfusion samples quantify eicosanoids in a rat model of skin inflammation. *J. Lipid Res.* 2019. 60: 758–766.

Supplementary key words prostaglandins • leukotrienes • liquid chromatography • tandem mass spectrometry • psoriasis • solid-phase extraction • microdialysis • lipid mediators

Eicosanoids are lipid-mediator molecules with key roles in fundamental biological processes such as inflammation (i.e., its promotion, suppression, or elimination) and homeostasis (1). Eicosanoids are endogenously derived from ω -3- and ω -6-PUFAs and released in the direct vicinity of an inflammation. Eicosanoids elicit local pleiotropic effects and dysregulations that occur in many severe diseases such as psoriasis, a common inflammatory skin disease (2–5). Psoriasis is a chronic, noninfectious, multifactorial disease that manifests foremost in scaling, erythematous plaques that often result in pruritus or pain (3, 6). Between 0.09% and 11.4% of the world population, i.e., more than 100 million people, are affected by psoriasis, rendering it a serious global health problem (7). The development of better psoriasis treatments requires a deeper understanding of disease pathogenesis and a better knowledge of the pharmacodynamics of topical or systemic treatments. The most relevant

This work was supported by the Federal Ministry of Transport, Innovation and Technology; the Federal Ministry of Science, Research and Economy; Land Steiermark; the Styrian Business Promotion Agency; and the Vienna Business Agency. During work on this publication C.P. and N.B. were employed at the Center for Biomarker Research in Medicine, C.P., B.R., T.B., F.S., M.B., and A.E. were employed at Joanneum Research Forschungsgesellschaft mbH, and K.E. and P.F. were employed at Sanofi. The employing companies provided support in the form of salaries, materials, and reagents and covered publication fees but did not influence decisions on study design, data analysis, or data interpretation.

Manuscript received 25 May 2018 and in revised form 25 January 2019.

Published, *JLR Papers in Press*, January 29, 2019

DOI <https://doi.org/10.1194/jlr.M087221>

Abbreviations: ACN, acetonitrile; CAV, cell accelerator voltage; CE, collision energy; CTRL, control; DEX, dexamethasone; dISF, dermal interstitial fluid; dOFM, dermal open-flow microperfusion; HLB, hydrophilic-lipophilic balance; IMQ, imiquimod; ISF, interstitial fluid; LTB₄, leukotriene B₄; MeOH, methanol; MRM, multiple reaction monitoring; OFM, open-flow microperfusion; PG, prostaglandin; QC, quality control; RSD, relative standard deviation; SPE, solid-phase extraction; TXB₂, thromboxane B₂; UHPLC, ultra-HPLC; 12-HEPE, 12-hydroxyeicosapentaenoic acid; 17-HDHA, 17-hydroxydocosahexaenoic acid.

¹To whom correspondence should be addressed.

e-mail: healthca@joanneum.at

^SThe online version of this article (available at <http://www.jlr.org>) contains a supplement.

Copyright © 2019 Pipper et al. Published under exclusive license by The American Society for Biochemistry and Molecular Biology, Inc.

This article is available online at <http://www.jlr.org>

data for new biomarkers, improved therapeutic regimens, or the identification of new therapeutic targets (8) are based on local monitoring of bioactive mediators such as eicosanoids directly at the main disease site: the skin. Unfiltered samples of dermal interstitial fluid (dISF) can be obtained most reliably by using minimally invasive dermal open-flow microperfusion (dOFM) technology with its membrane-free design (9, 10), but dOFM samples provide only a very limited volume depending on sampling time.

In general, eicosanoids in biological samples can be analyzed with classic analytical methods, including immunological methods (RIA, ELISA); newer GC/MS methods; and, more recently, derivatization-free LC/MS methods, which enable more robust quantification and simpler handling (11–13). Various eicosanoid LC/MS methods for sample types such as plasma or urine samples are well established (14–17), and methods for blood (18), tissue (19), or cell-culture supernatants (20, 21) have been successfully implemented. These sample types provide higher volumes and eicosanoid concentrations relative to dISF samples. Analyzing eicosanoids from dISF is challenging due to the small available volumes, matrix, often very low endogenous eicosanoid concentration, isomeric nature, and limited chemical stability of some eicosanoids. So far, dISF samples have been used in only one LC/MS study that specifically studied the effect of UVB irradiation and diclofenac on three specific eicosanoids (22). Other eicosanoids that could be relevant for inflammatory skin diseases in general and psoriasis in particular are not covered by this method and were thus targeted in our study.

We aimed to establish a quickly transferable, simple, and expandable LC/MS method for a highly sensitive and robust quantification of relevant eicosanoids. The *in vivo* applicability of the method was verified in a pilot rat study using local inflammation triggered by topical imiquimod (IMQ). Furthermore, we investigated the impact of the orally administered anti-inflammatory corticosteroid dexamethasone (DEX) on the eicosanoid pattern in IMQ-treated and untreated skin sites.

MATERIALS AND METHODS

Thromboxane B₂ (TXB₂), prostaglandin (PG) E₂, PGD₂, PGF_{2α}, leukotriene B₄ (LTB₄), 15-HETE, 12-HETE, 5-HETE, 17-hydroxydocosahexaenoic acid (17-HDHA), 13-HODE, 12-hydroxyeicosapentaenoic acid (12-HEPE), and the multiple deuterated internal standards TXB₂-d₄, PGE₂-d₄, PGD₂-d₄, PGF_{2α}-d₄, LTB₄-d₄, 15(*S*)-HETE-d₈, 12(*S*)-HETE-d₈, 5(*S*)-HETE-d₈, and 13(*S*)-HODE-d₄ were purchased from Cayman Chemicals (Ann Arbor, MI).

All solvents [2-propanol, acetonitrile (ACN), methanol (MeOH), ethanol, ethyl acetate] were obtained from Sigma-Aldrich (St. Louis, MO). Reagent-grade formic acid was from Agilent Technologies (Waldbronn, Germany). ELO-MEL isoton was obtained from Fresenius Kabi (Bad Homburg vor der Höhe, Germany). Water was purified with a MilliQ system (Millipore GmbH, Vienna, Austria).

Sample preparation

The sample preparation was optimized in terms of minimal preanalytical loss of the targeted eicosanoids. All dOFM samples

were thawed on ice while protected from light; 180 µl of the dOFM sample, standard solutions, or blanks were diluted with 400 µl 10% MeOH, and 0.1% formic acid in water solution and 15 µl of the diluted internal standard mix (10 ng/ml) were added.

Each internal standard was diluted stepwise using the required amount of the original standard. For the first dilution step, ethanol was used to reach a concentration of 10 µg/ml for each internal standard. All stocks were overlaid with argon and kept at –80°C in amber glass vials until usage. Mobile phase A was used for further dilution to gain a concentration of 100 ng/ml for all internal standards in the mix, which was then diluted 1:10 using mobile phase A to reach a concentration of 10 ng/ml. This mix was prepared shortly before starting the analytical process and kept at –80°C until usage; 15 µl of this dilution was added to the sample mix and to the calibration and quality control (QC) samples just before the solid-phase extraction (SPE). The QC samples were a mix of each eicosanoid and the deuterated internal standards at 0.5, 5, or 25 ng/ml in the isotonic saline ELO-MEL; 180 µl of the eicosanoid mix was diluted with 400 µl 10% MeOH and 0.1% formic acid solution before 15 µl of the internal standard mix (10 ng/ml) was added. After thorough vortexing, the diluted mix was loaded onto the conditioned and equilibrated SPE. The SPE was then used to concentrate and clean the interstitial fluid (ISF) samples. For this an Oasis hydrophilic-lipophilic balance (HLB) 96-well µElution plate (2 mg sorbent per well; 30 µm particle size) was used in combination with an extraction-plate manifold for Oasis 96-well plates (Waters, Milford, MA) and a vacuum pump system (DOA-V517-BN; Gast Manufacturing Inc., Benton Harbor, MI).

SPE plates were briefly conditioned with 200 µl MeOH and equilibrated with 200 µl 0.1% formic acid in water. After equilibration, the diluted samples were loaded and washed with 200 µl 5% MeOH in water. Eicosanoids were eluted with 50 µl MeOH, and 50 µl ethyl acetate was then loaded into a 1,000 µl 96-well Protein LoBind Plate (Eppendorf, Hamburg, Germany). Eluted samples were dried under a N₂ stream at room temperature (MiniVap; 96 needle heads; Porvair Sciences, Wrexham, UK). Samples were resuspended in 30 µl mobile phase A, which was cautiously overlaid with argon gas and sealed (sealing mat for DWP 96/1000; Eppendorf). Plates were agitated with a Titramax 100 (Heidolph Instruments, Schwabach, Germany) at 1,050 rpm for 15 min at 22°C prior to analysis.

ULTRA-HPLC/MS/MS

All separations were performed using a 1290 Infinity II LC System (Agilent Technologies). For optimal chromatographic separation, a Waters Acquity UPLC BEH C₁₈ column (2.1 × 150 mm; 1.7 µm particle size) was used in combination with a VanGuard Pre-column (Waters). The column temperature was 30 ± 5°C, the injection volume was 7.5 µl, and the flow rate was 0.3 ml/min with a run time of 16 min. Mobile phases were degassed for 5 min with a SONOREX RK 100 (Bandelin, Berlin, Germany). Mobile phase A was water-ACN-formic acid (63:37:0.02; v/v/v), and mobile phase B was ACN:2-propanol (50:50; v/v). The gradient elution was as follows: 0–6.0 min 0% B; 6.0–6.5 min 0% to 55% B; 6.5–10.0 min 55% B; 10.0–12.0 min 55% to 100% B; 12.0–13.0 min 100% B; 13.0–13.5 min 100% to 0% B; and 13.5–16.0 min 0% B.

Mass detection was performed in dynamic multiple reaction monitoring (dMRM) mode with an Agilent 6495 triple quadrupole system equipped with Agilent Jet Stream thermal gradient focusing technology, which uses an enhanced ESI technique and super-heated nitrogen sheath gas to confine the nebulizer spray. As a result, the ions are desolvated and concentrated near the MS inlet (23). Negative ionization was used, the capillary voltage was 3 kV, and the nozzle voltage was 500 V. The source was operated at 240°C with a gas flow of 13 l/min, and the sheath gas was set at 360°C with a flow rate of 12 l/min. A pressure of 30 psi

TABLE 1. dMRM transitions, retention time, Δ retention time, CEs, and CAVs of the eicosanoids and the deuterated internal standards

Compound	Precursor Ion > Product Ion	Retention Time (min)	Δ Retention Time (min)	CE	CAV
TXB ₂	369.2 > 169.0	3.5	2	13	3
TXB ₂ -d4	373.3 > 173.1	3.5	2	13	3
PGF _{2α}	353.2 > 193.0	4.3	2	25	3
PGF _{2α} -d4	357.3 > 197.1	4.3	2	25	3
PGE ₂	351.2 > 189.1	5.1	4	17	3
PGE ₂ -d4	355.2 > 193.2	5.1	4	21	3
PGD ₂	351.2 > 189.1	6.0	4	17	3
PGD ₂ -d4	355.2 > 193.2	6.0	4	17	3
LTB ₄	335.2 > 195.0	8.9	4	17	3
LTB ₄ -d4	339.2 > 197.1	8.9	2	17	3
12-HEPE	317.2 > 179.0	9.9	2	13	3
13-HODE	295.5 > 195.1	10.2	2	17	3
13(S)-HODE-d4	299.5 > 198.0	10.2	2	17	3
17-HDHA	343.5 > 280.8	10.5	2	9	3
15-HETE	319.2 > 219.0	10.7	2	13	3
15(S)-HETE-d8	327.3 > 226.2	10.7	2	13	3
12-HETE	319.2 > 179.0	10.8	2	13	3
12(S)-HETE-d8	327.3 > 184.1	10.8	2	13	3
5(S)-HETE-d8	327.3 > 116.0	11.4	2	13	3
5-HETE	319.2 > 115.0	11.4	2	13	3

was applied to the nebulizer. See Table 1 for specific eicosanoid settings.

Rat study design and dOFM sampling

Local skin inflammation was studied in a total of 12 adult male Sprague-Dawley rats (Charles River Laboratories, Wilmington, MA). Each rat was treated daily on one side of its back with Imiquimod Cream 5% (Fougera Pharmaceutical Inc., Melville, NY) to induce local skin inflammation (IMQ group), and the other side was left untreated [control (CTRL) group]. Six rats received an additional oral DEX treatment (2 mg/kg body weight per day) to suppress inflammation (IMQ-DEX group, DEX group). dISF was collected with three dOFM probes placed in the IMQ-treated site of each rat, and three dOFM probes were placed in the untreated,

noninflamed site on the other side of the back (Fig. 1). dOFM sampling was performed under general anesthesia following a previously published protocol (24).

dISF samples were collected in 0.2 ml PCR tubes (Protein Lo-Bind quality; PCR-02-L-L; Axygen Scientific, Tewksbury, MA) and cooled in custom-fit ice-filled beakers. Tubes and ice beakers were changed every 2 h, and the samples were refrigerated at 4°C throughout the entire 8 h sampling period. After sampling, all aliquots from one site (three dOFM probes) were pooled and immediately frozen at -20°C. Samples were transferred within 1 day to -80°C for storage until analysis.

All animal experiments were approved by the Austrian federal government and performed in accordance with Directive 2010/63/EU.

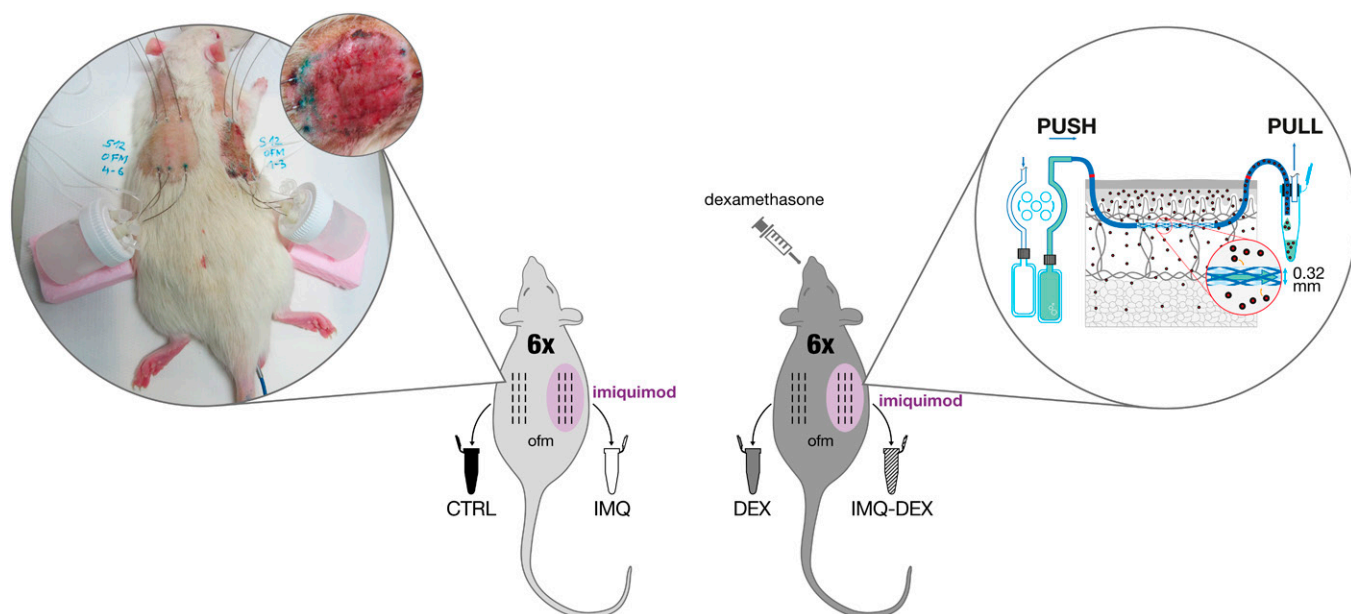


Fig. 1. dOFM study design. All rats were treated with topical IMQ on one side of the back to induce local inflammation. In addition, 6 of the 12 rats received systemic oral DEX treatment. Samples were collected from each side with three dOFM probes. The magnified right part of the figure shows a schematic representation of the dOFM sampling used (10, 56), demonstrating the collection of diluted ISF directly from the skin; the image on the left shows a rat during sampling and a close-up of the IMQ-treated test site.

Statistical analysis

Statistical analysis was performed with R version 3.4 packages *lawstat* (25), *nlme* (26), and *lsmeans* (27) and Tibco Spotfire version 7.5. ANOVAs were calculated with *lme*, and post hoc pairwise group comparisons were calculated with *lsmeans*. Duplicate concentrations were averaged, and results were found to be insufficiently normally distributed as well as heteroscedastic. Afterward, \log_{10} transformation data were sufficiently normally distributed according to a Kolmogorov-Smirnov test and sufficiently homoscedastic according to a Brown-Forsythe Levene-type test (supplemental data S1).

The study design was balanced, had no missing values, and contained two fixed factors (IMQ and DEX) and *subject_ID* as a random factor nested within the factor DEX. In total, six plausible different models were tested and selected according to quality of fit, significance of factors, degrees of freedom, Akaike information criterion, log-likelihood, distribution of residuals, and quantile-quantile plots (supplemental data S1). Results from the two best models, the simple (\sim IMQ \times DEX) and mixed random slope (\sim IMQ \times DEX, random = \sim I + DEX \times IMQ | *subject_ID*) models, were analyzed, and *P* values were adjusted by Benjamini-Hochberg for multiple testing (per model). Results from both models overlapped well, and results from the random slope model are presented because the literature recommends using

multilevel analysis for dependent and nested data and because a random slope is more biologically plausible and achieves better log-likelihood with often smaller or similar Akaike information criterion (28).

RESULTS AND DISCUSSION

Method development and validation

For sample preparation, we used SPE, which is one of the most commonly used preparation techniques (20). Compared with liquid-liquid extraction, SPE offers reduced impurities, ease of use for higher sample numbers, and the possibility of concentrating samples. Selecting suitable SPEs is straightforward, and we briefly compared two systems, the Oasis HLB SPE and the Oasis MAX SPE (Waters). The HLB SPE achieved notably better recovery and precision and was subsequently used for all experiments (data not shown).

High recovery rates with low relative standard deviation (RSD) in one SPE run were difficult to achieve because of the chemical diversity of the studied eicosanoids. Therefore,

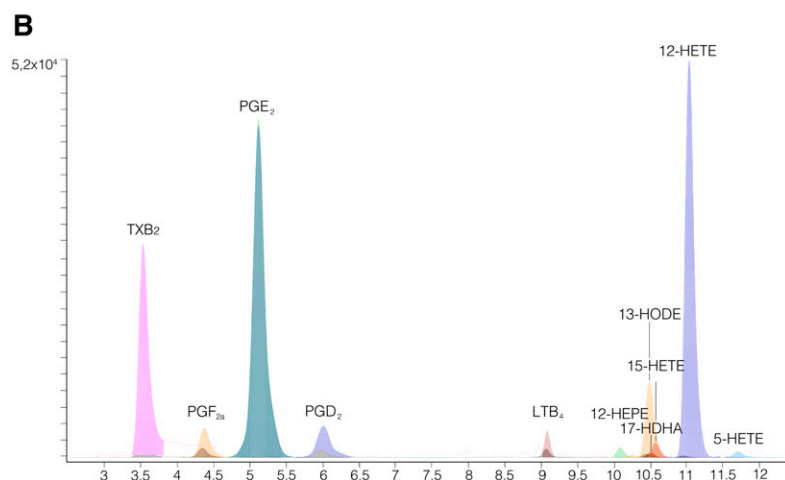
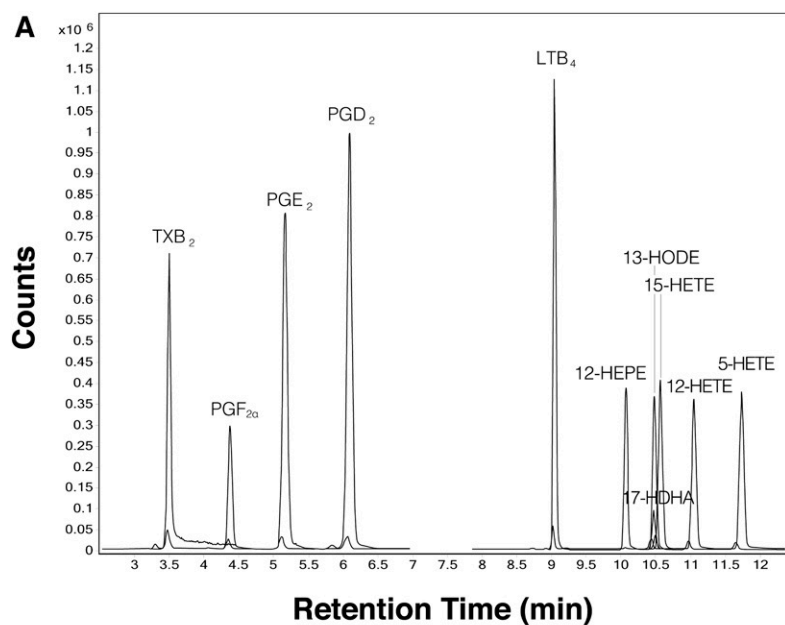


Fig. 2. A: Representative UHPLC-dMRM chromatogram of the targeted 11 eicosanoids and the corresponding internal standards (Table 1). B: Representative UHPLC-dMRM chromatogram of the targeted 11 eicosanoids and the corresponding internal standards from a diluted interstitial fluid sample. The small darker peaks represent the internal standards.

we added nine deuterated internal standards to each sample before extraction to enable robust, highly sensitive quantification and to compensate for potential losses during sample preparation.

Special emphasis had to be placed on good chromatographic separation because some of the targeted eicosanoids are isomeric. The Agilent ultra-HPLC (UHPLC) system showed the best chromatographic performance of all of our tested systems for all targeted eicosanoids. An exemplary chromatographic separation of a standard mix is provided in **Fig. 2**. A chromatogram of an ISF sample is presented in **Fig. 2A**, and the selected ion recordings of each single analyte and corresponding internal standard are provided in supplemental **Fig. S1**. The method was not shortened further to leave some time slots in the chromatogram for potential future expansion of the eicosanoid panel.

Negative ionization was used for detection, taking advantage of the terminal carboxyl moiety of the eicosanoids. dMRM was used to monitor multiple transitions simultaneously. Literature data and the Agilent optimizer tool (part of the MassHunter software package) were used to select product ions, collision energies (CEs), and cell accelerator voltages (CAVs) (8, 14–17, 29–33). Final settings are provided in **Table 1**. Due to the two-stage *m/z* selection an enhancement of the analytical selectivity and improved signal-to-noise ratios were achieved. Monitoring of precursors

TABLE 2. Linearity between LOD and 50 ng/ml for the 11 eicosanoids

Compound	Goodness of Fit (R^2)	LOD (ng/ml)	Concentrations in Linear Fit (<i>n</i>)
TXB ₂	0.997	0.01	12
PGF _{2α}	0.998	0.01	12
PGE ₂	0.998	0.01	12
PGD ₂	0.995	0.01	12
LTB ₄	0.999	0.25	9
12-HEPE	0.990	0.01	12
17-HDHA	0.980	0.1	10
13-HODE	0.997	0.01	12
15-HETE	0.998	0.01	12
12-HETE	0.997	0.01	12
5-HETE	0.994	0.025	11

as well as specific, abundant product ions is usually performed to maximize sensitivity in LC/MS/MS eicosanoid analysis (20). The usage of dMRM provided further sensitivity compared with multiple reaction monitoring and full scan.

For method validation, we also assessed the linearity of calibration curves and the accuracy and precision of quantification. Calibration curves were selected to cover most eicosanoid concentrations and the low concentrations to be expected in such diluted material as ISF from dOFM (20). For each eicosanoid, 12 calibration points ranging from 0.01 to 50 ng/ml were measured. This calibration range covered the in vivo concentrations very well, except for 12-HETE, which was found to have concentrations >50

TABLE 3. Exemplary intra- and interday precisions and accuracy

Compound	Intraday Day 1 (<i>n</i> = 6)			Intraday Day 2 (<i>n</i> = 12)			Interday (<i>n</i> = 18)		
	Measured (ng/ml)	RSD (%)	Accuracy (%)	Measured (ng/ml)	RSD (%)	Accuracy (%)	Measured (ng/ml)	RSD (%)	Accuracy (%)
TXB ₂	0.51	±5.20	102.85	0.46	±6.04	91.45	0.48	±8.05	95.25
	5.13	±7.26	102.69	4.75	±5.37	94.92	4.88	±7.06	97.51
	23.25	±3.18	92.99	25.49	±8.19	101.97	24.74	±8.25	98.98
PGF _{2α}	0.53	±5.55	106.38	0.44	±6.57	88.14	0.47	±11.14	94.22
	4.89	±2.47	97.86	4.50	±5.62	89.93	4.63	±6.20	92.58
	24.63	±3.68	98.50	24.57	±3.25	98.27	24.59	±3.29	98.35
PGE ₂	0.47	±3.52	93.28	0.45	±1.17	90.73	0.46	±2.54	91.58
	4.52	±2.32	90.38	4.59	±3.50	91.75	4.56	±3.18	91.29
	22.61	±2.22	90.44	25.54	±3.81	102.14	24.56	±6.69	98.24
PGD ₂	0.39	±10.64	77.38	0.44	±6.37	87.93	0.42	±9.66	84.42
	3.94	±8.60	78.70	4.59	±4.68	91.81	4.37	±9.28	87.44
	20.85	±9.73	83.38	25.01	±5.68	100.04	23.62	±10.87	94.49
LTB ₄	0.53	±1.76	105.71	0.38	±6.48	76.21	0.43	±17.30	86.04
	5.25	±1.60	104.90	4.02	±4.30	80.40	4.43	±13.82	88.56
	27.11	±2.05	108.44	23.81	±1.69	95.23	24.91	±6.68	99.63
12-HEPE	0.40	±9.41	79.81	0.40	±3.59	79.19	0.40	±5.89	79.39
	3.74	±11.61	74.88	3.74	±2.90	74.88	3.74	±6.71	74.88
	20.30	±10.16	81.22	23.69	±3.79	94.77	22.56	±9.37	90.25
17-HDHA	0.37	±9.26	74.73	0.39	±8.23	77.07	0.38	±8.44	76.29
	3.71	±9.35	74.23	3.39	±7.11	67.88	3.50	±8.89	70.00
	20.84	±8.78	83.36	22.88	±3.22	91.52	22.20	±6.85	88.80
13-HODE	0.44	±4.08	88.36	0.40	±6.84	79.95	0.41	±7.63	82.75
	4.42	±4.72	88.42	3.86	±5.35	77.11	4.04	±8.41	80.88
	23.38	±4.05	93.52	23.76	±3.54	95.03	23.63	±3.67	94.53
15-HETE	0.38	±3.93	75.96	0.40	±5.11	79.62	0.39	±5.18	78.40
	4.03	±3.24	80.53	3.79	±5.87	75.87	3.87	±5.77	77.42
	21.51	±2.29	86.04	23.69	±3.59	94.75	22.96	±5.60	91.84
12-HETE	0.34	±2.16	67.35	0.39	±4.60	78.53	0.37	±8.29	74.81
	3.64	±3.19	72.71	3.58	±8.96	71.61	3.60	±7.42	71.98
	20.32	±2.92	81.29	22.65	±3.10	90.61	21.88	±5.96	87.50
5-HETE	0.38	±6.31	75.36	0.48	±9.35	95.19	0.44	±13.84	88.58
	3.65	±2.84	73.07	3.71	±9.88	74.21	3.69	±8.16	73.83
	18.99	±2.96	75.98	22.30	±4.22	89.20	21.20	±8.49	84.79
Median		3.9	83.4		5.1	89.9		7.6	88.6

ng/ml in some samples that were determined by extrapolation (maximum: 123.5 ng/ml). The lowest acceptable calibration curve point was selected by signal-to-noise ratios ≥ 10 (Table 2) based on data found in the literature (34–37). The differences in the lowest limit for detecting the different eicosanoids can most likely be attributed to differences in ionization efficiency rather than to matrix effects because SPE-based sample preparation is known to provide very clean extracts (38).

The stable-isotope dilution method was used for eicosanoid quantification and resulted in a linear standard curve when plotting relative concentration (x ; the ratio between analyte and stable isotope-labeled compound) against relative response (y). These calibration curves were fitted by a weighted ($1/x$) least-squares regression (MassHunter). Regarding linearity, 10 of 11 eicosanoids achieved an excellent average ($n = 6$) $R^2 > 0.994$, and even 17-HDHA had a very good linearity ($R^2 = 0.980$; Table 2).

Three QC samples with different concentrations were measured in six replicates on the same day, and 12 replicates were measured on the next day for intra- and interday accuracy and precision. Accuracy was calculated as the percentage of measured concentration relative to nominal concentration, whereas the precision is reported as relative standard deviation (RSD). According to US Federal Drug and Administration standards, precision and accuracy were found to be satisfactory overall (Table 3). High median intraday precision across all eicosanoids was achieved with 3.9% and 5.1%. As expected, median interday precision was slightly inferior (7.6%) compared with intraday precision. Intra- and interday accuracy was similar, with a median for all eicosanoids of approximately 85% (83.4% day 1, 89.9% day 2, 88.6% interday day 1 vs. day 2). Accuracy tended to be superior for eicosanoids that had higher SPE recovery.

In summary, we established a robust and sensitive method for quantifying all 11 tested eicosanoids. Extraction recovery differed among the investigated eicosanoids but was always sufficient, and extraction precision was consistent. The linearity of calibration curves was excellent, and precision as well as accuracy differed among the analytes, but both parameters were always more than sufficient for applying this quantification method in an open-flow microperfusion (OFM) setup.

Method application

The application of our validated analytical method was tested by using dISF samples obtained from rat skin during a preclinical skin inflammation study (39). Psoriasis-like skin inflammation was successfully induced by IMQ treatment (Fig. 1), with a skinfold thickness ranging from 1.99 ± 0.09 (IMQ-DEX) to 2.02 ± 0.1 mm (DEX) and 2.59 ± 0.17 (CTRL) to 5.1 ± 0.65 mm (IMQ). Erythema and scaling scored zero for CTRL, DEX, and IMQ-DEX compared with 1.67 ± 0.52 and 1.67 ± 1.03 , respectively, for IMQ-treated sites. Minimally invasive OFM sampling yields dISF samples that require optimized analytical strategies for small sample volumes (9, 39, 40). In a total of 24 samples from 12 rats, 11 eicosanoids were

quantified. The measured eicosanoids were selected according to results from various published studies on humans (3, 41–43).

The chosen inflammatory agent IMQ is a potent immune activator and synthetic toll-like receptor 7/8 ligand that induces skin inflammation through toll-like receptor 7 ligation and exacerbates the condition in patients with psoriasis (44–46). Even in patients with no prior history of psoriasis, IMQ has been shown to induce psoriasis development (47). IMQ has previously been used to induce psoriasis-like skin conditions in mice (45, 46, 48–52) and rats (39, 40, 53, 54) and is expected to induce inflammation mediators such as eicosanoids. Oral treatment with the strong anti-inflammatory glucocorticoid DEX (Fig. 1) was expected to decrease eicosanoid levels. To investigate the overall effects of IMQ and DEX treatment, we plotted the summarized concentrations of all eicosanoids (Fig. 3). Because the absolute concentrations of single eicosanoids differed by orders of magnitudes (e.g., 12-HETE had on average a 50 times higher concentration in the IMQ group relative to 12-HEPE, 15-HETE, 17-HDHA, and others), the summed absolute concentrations would be dominated by the two most abundant eicosanoids, 12-HETE and 13-HODE,

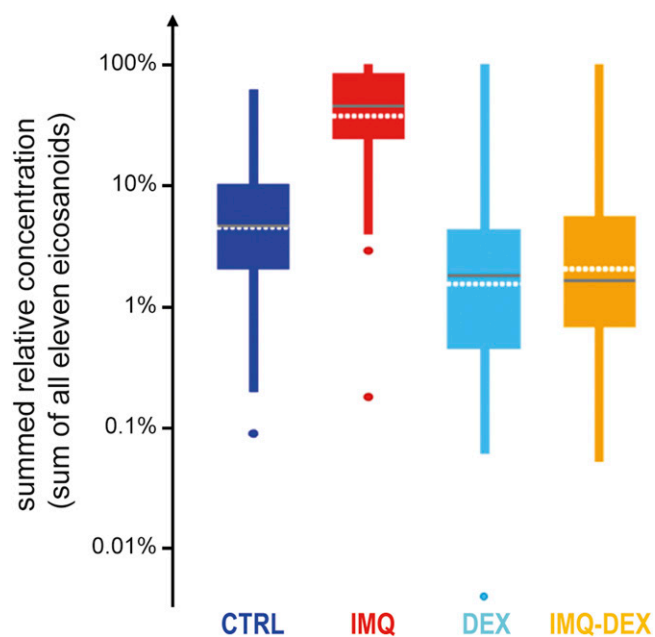


Fig. 3. Overview of eicosanoid concentrations in rats as a sum of relative concentrations in one sample per treatment group. The relative concentration for each eicosanoid in each sample was calculated by scaling each eicosanoid to a scale from 0 to 1 as follows: $\text{relative concentration}_{\text{eicosanoid in sample}} = (\text{absolute concentration}_{\text{eicosanoid in sample}} - \text{minimal concentration}_{\text{eicosanoid in all samples}}) / (\text{maximal concentration}_{\text{eicosanoid in all samples}} - \text{minimal concentration}_{\text{eicosanoid in all samples}})$. The sum of all relative concentrations is plotted in a logarithmic scale for the four groups: CTRL (no treatment), IMQ (topical IMQ treatment), DEX (systemic DEX treatment), and DEX-IMQ (systemic DEX and topical IMQ treatment). Dots indicate outside values; ends of lines indicate either the upper and lower adjacent value, respectively; the top and bottom of the box indicate the upper and lower quartile, respectively; the horizontal gray line indicates the median; and the horizontal white dotted line indicates the average.

representing ~83% of the absolute concentrations. This would render potentially different behavior of all other eicosanoids invisible in the summed plot. However, the biological impact and importance of one eicosanoid compared with another does not necessarily depend on the difference of absolute concentrations between them but rather on their relative changes and activated subsequent pathways. Consequently, relative concentrations were summed so that each eicosanoid concentration contributed equally (see legend to Fig. 3). As expected, overall relative eicosanoid concentrations were highly increased in IMQ sites compared with CTRL sites, while DEX treatment successfully suppressed the eicosanoid response to inflammation (Fig. 3). Single eicosanoid box plots are shown in Fig. 4, and the corresponding ratios and *P* values are provided in supplemental data S1.

A detailed analysis of individual eicosanoid concentrations showed a significant increase in IMQ sites compared with CTRL sites, except for 13-HODE, where the increase was not significant. Compared with previous studies on humans in which HODE was found to be significantly increased in human psoriatic skin scales (55), no studies have yet reported an increase in HODE in rats. Our results are also in line with observations in studies on humans reporting an increase in PGE₂ (42), but the role and importance of PGE₂ in psoriasis are still debated (3). Although physiological concentrations of active 12-HETE, 15-HETE, and LTB₄ have been described in human lesional skin, a comprehensive pathophysiological analysis of these interacting eicosanoids for psoriatic lesions is not yet available. The role of other eicosanoids such as LTB₄ and 12-HETE has been described in more detail. Both have chemoattractant and mitogenic effects in the skin and thus very likely play key roles in the pathophysiology of inflamed skin. 15-HETE takes the role of the antagonist and may act as an important

regulator in LTB₄- and 12-HETE-induced inflamed sites (3). Such a comprehensive analysis of interacting eicosanoids is supported by using a combination of OFM sampling and LC/MS, which provides new data directly from the tissue for a better understanding of the pathophysiology in inflammatory lesions.

Other eicosanoids derived from cyclooxygenase and lipoxygenase pathways that showed an increase in our rat model, including TXB₂, PGF_{2α}, PGD₂, 13-HODE, 17-HDHA, 12-HEPE, and 5-HETE, have previously been described to also play important roles in inflammatory and anti-inflammatory processes in the skin (4, 43). The consistent pattern of increased eicosanoid concentrations after inflammation in human as well as animal models supports the importance of measuring eicosanoids directly from lesional skin to gain deeper mechanistic insights.

Regarding the suppression of the inflammatory response, sampling sites in rats treated with DEX yielded lower eicosanoid concentrations compared with completely untreated sites (Fig. 3). This pattern confirms the strong anti-inflammatory effect of glucocorticosteroids that are routinely used for the treatment of various autoimmune diseases, allergic reactions, and many other diseases. All eicosanoids concentrations were lower in the IMQ-DEX sites than in the IMQ sites, with 8 of 11 being significantly lowered (Fig. 4, orange vs. red). The suppressing impact of glucocorticoids on arachidonic acid and HETEs in treatments of inflammatory skin diseases has long been known (41). The applied anti-inflammatory treatment was even strong enough to significantly lower the endogenous eicosanoid levels of five eicosanoids in the DEX-treated rats (Fig. 4, light blue vs. blue). Despite the very strong anti-inflammatory effect of DEX, three eicosanoids (12-HEPE, 12-HETE, and PGE₂) still showed a significant increase in IMQ-treated sites, with ratios between 1.2 and 1.6 compared

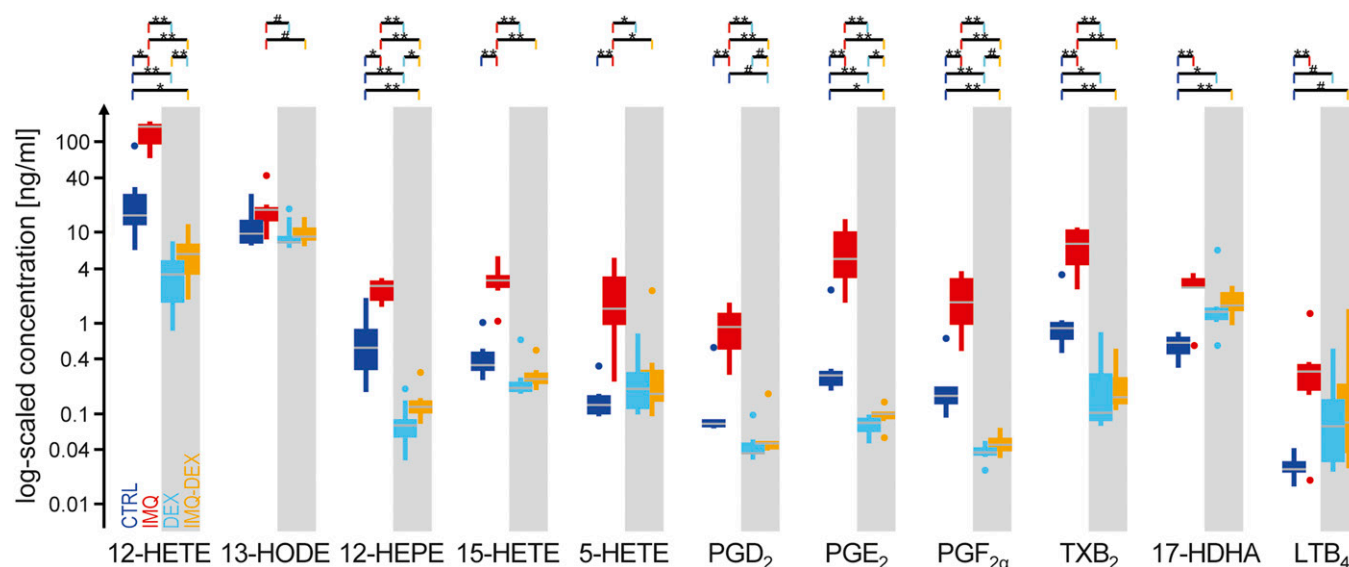



Fig. 4. Box plots of all 11 quantified eicosanoids in 12 rats. Concentrations are plotted in a logarithmic scale. The white background indicates the group with only IMQ treatment (*n* = 6); the gray background indicates the group with systematic DEX treatment (*n* = 6). Dots indicate outside values; ends of lines indicate either the upper and lower adjacent value, respectively; the top and bottom of the box indicate the upper and lower quartile, respectively; and the middle gray line indicates the median. ***P* < 0.01, **P* < 0.05, and #*P* < 0.1.

with untreated skin sites in the same group of rats (Fig. 4, orange vs. light blue), indicating that even strong glucocorticoid therapy can fail to fully block inflammatory mediator production in rats. Our results can contribute to a better understanding of the therapeutic effect of steroid therapies in skin diseases and underline the importance of intralésional measurements for further mechanistic insights.

In summary, 11 eicosanoid concentrations were well measurable in small-volume samples with the developed method, and differences in concentrations under various treatments corresponded perfectly to expectations.

CONCLUSIONS

The established method for quantifying eicosanoids was sensitive, reproducible, precise, accurate, robust, and well applicable to rat dISF samples. The provided degree of detail aims to ease the adoption of this method in other labs, and the implemented chromatographic separation allows the addition of further analytes. This method can be applied to other biological materials with just minor adaptations and is especially well suited for the analysis of small-volume samples or diluted solutions. Using this analytical method, we were able to measure the expected increase in eicosanoid concentrations after the induction of skin inflammation and to determine significant differences compared with untreated skin as well as the suppressing impact of corticosteroid treatment. This exemplifies how measuring inflammatory mediators such as eicosanoids directly at the main disease site, i.e., the skin, can contribute toward a better understanding of pathogenesis, pharmacodynamics, and treatment responses. 

The authors thank Sonja Kainz, Simon Schwingenschuh, Jürgen Lanczaj, Peter Reisenegger, and Günther Rauter for supporting and performing the animal experiments; Bianca Kranz for assistance in graphic design; and Selma Mautner for critical review and editorial assistance.

REFERENCES

- Galvão, A. F., T. Petta, N. Flamand, V. R. Bollela, C. L. Silva, L. R. Jarduli, K. C. R. Malmegrim, B. P. Simões, L. A. B. de Moraes, and L. H. Faccioli. 2016. Plasma eicosanoid profiles determined by high-performance liquid chromatography coupled with tandem mass spectrometry in stimulated peripheral blood from healthy individuals and sickle cell anemia patients in treatment. *Anal. Bioanal. Chem.* **408**: 3613–3623.
- Ikai, K. 1999. Psoriasis and the arachidonic acid cascade. *J. Dermatol. Sci.* **21**: 135–146.
- Fogh, K., and K. Kragballe. 2000. Eicosanoids in inflammatory skin diseases. *Prostaglandins Other Lipid Mediat.* **63**: 43–54.
- Kendall, A. C., and A. Nicolaou. 2013. Bioactive lipid mediators in skin inflammation and immunity. *Prog. Lipid Res.* **52**: 141–164.
- Dennis, E. A., and P. C. Norris. 2015. Eicosanoid storm in infection and inflammation. *Nat. Rev. Immunol.* **15**: 511–523.
- Jiang, S., T. E. Hinchliffe, and T. Wu. 2015. Biomarkers of an autoimmune skin disease—psoriasis. *Genomics Proteomics Bioinformatics.* **13**: 224–233.
- World Health Organization. 2016. Global Report on Psoriasis. World Health Organization, Geneva, Switzerland.
- Massey, K. A., and A. Nicolaou. 2013. Lipidomics of oxidized polyunsaturated fatty acids. *Free Radic. Biol. Med.* **59**: 45–55.
- Bodenlenz, M., B. Aigner, C. Dragatin, L. Liebenberger, S. Zahiragic, C. Höfner, T. Birngruber, J. Priedl, F. Feichtner, L. Schaupp, et al. 2013. Clinical applicability of dOFM devices for dermal sampling. *Skin Res. Technol.* **19**: 474–483.
- Dragatin, C., F. Polus, M. Bodenlenz, C. Calonder, B. Aigner, K. I. Tiffner, J. K. Mader, M. Ratzner, R. Woessner, T. R. Pieber, et al. 2016. Secukinumab distributes into dermal interstitial fluid of psoriasis patients as demonstrated by open flow microperfusion. *Exp. Dermatol.* **25**: 157–159.
- Eberl, A., and F. Sinner. 2018. Liquid chromatography-mass spectrometry of eicosanoids. In *Encyclopedia of Lipidomics*. M. R. Wenk, editor. Springer, Dordrecht, the Netherlands. doi:10.1007/978-94-007-7864-1.
- Tsikas, D., and A. A. Zoerner. 2014. Analysis of eicosanoids by LC-MS/MS and GC-MS/MS: a historical retrospect and a discussion. *J. Chromatogr. B Analyt. Technol. Biomed. Life Sci.* **964**: 79–88.
- Astarita, G., A. C. Kendall, E. A. Dennis, and A. Nicolaou. 2015. Targeted lipidomic strategies for oxygenated metabolites of polyunsaturated fatty acids. *Biochim. Biophys. Acta.* **1851**: 456–468.
- Ostermann, A. I., I. Willenberg, and N. H. Schebb. 2015. Comparison of sample preparation methods for the quantitative analysis of eicosanoids and other oxylipins in plasma by means of LC-MS/MS. *Anal. Bioanal. Chem.* **407**: 1403–1414.
- Rago, B., and C. Fu. 2013. Development of a high-throughput ultra performance liquid chromatography-mass spectrometry assay to profile 18 eicosanoids as exploratory biomarkers for atherosclerotic diseases. *J. Chromatogr. B Analyt. Technol. Biomed. Life Sci.* **936**: 25–32.
- Shinde, D. D., K-B. Kim, K-S. Oh, N. Abdalla, K-H. Liu, S. K. Bae, J-H. Shon, H-S. Kim, D-H. Kim, and J. G. Shin. 2012. LC-MS/MS for the simultaneous analysis of arachidonic acid and 32 related metabolites in human plasma: basal plasma concentrations and aspirin-induced changes of eicosanoids. *J. Chromatogr. B Analyt. Technol. Biomed. Life Sci.* **911**: 113–121.
- Zhang, X., N. Yang, D. Ai, and Y. Zhu. 2015. Systematic metabolomic analysis of eicosanoids after omega-3 polyunsaturated fatty acid supplementation by a highly specific liquid chromatography-tandem mass spectrometry-based method. *J. Proteome Res.* **14**: 1843–1853.
- Song, J., X. Liu, J. Wu, M. J. Meehan, J. M. Blevitt, P. C. Dorrestein, and M. E. Milla. 2013. A highly efficient, high-throughput lipidomics platform for the quantitative detection of eicosanoids in human whole blood. *Anal. Biochem.* **433**: 181–188.
- Yue, H., S. A. Jansen, K. I. Strauss, M. R. Borenstein, M. F. Barbe, L. J. Rossi, and E. Murphy. 2007. A liquid chromatography/mass spectrometric method for simultaneous analysis of arachidonic acid and its endogenous eicosanoid metabolites prostaglandins, dihydroxyeicosatrienoic acids, hydroxyeicosatetraenoic acids, and epoxyeicosatrienoic acids in rat br. *J. Pharm. Biomed. Anal.* **43**: 1122–1134.
- Martin-Venegas, R., O. Jáuregui, and J. J. Moreno. 2014. Liquid chromatography-tandem mass spectrometry analysis of eicosanoids and related compounds in cell models. *J. Chromatogr. B Analyt. Technol. Biomed. Life Sci.* **964**: 41–49.
- Yang, R., N. Chiang, S. F. Oh, and C. N. Serhan. 2011. In *Current Protocols in Immunology*. John Wiley & Sons, Inc., Hoboken, NJ. Chapter 14, 1–36.
- Wiswedel, I., J-U. Grundmann, M. Boschmann, A. Krautheim, R. Böckelmann, D. S. Peter, I. Holzapfel, S. Götz, C. Müller-Goymann, B. Bonnekoh, et al. 2007. Effects of UVB irradiation and diclofenac on F2-isoprostane/prostaglandin concentrations in keratinocytes and monodialsates of human skin. *J. Invest. Dermatol.* **127**: 1794–1797.
- Mordehai, A., and J. Fjeldsted. 2009. Agilent Jet Stream Thermal Gradient Focusing Technology. Agilent Technologies, Santa Clara, CA.
- Höfner, C., D. Tutkur, C. Fledelius, C. L. Brand, T. J. Alsted, J. Damgaard, E. Nishimura, C. B. Jeppesen, S. I. Mautner, T. R. Pieber, et al. 2015. Open flow microperfusion: pharmacokinetics of human insulin and insulin detemir in the interstitial fluid of subcutaneous adipose tissue. *Diabetes Obes. Metab.* **17**: 121–127.
- Gastwirth, J. L., Y. R. Gel, W. L. W. Hui, V. Lyubchich, W. Miao, and K. Noguchi. 2015. lawstat: Tools for biostatistics, public policy, and law. Accessed June 27, 2017, at <https://rdr.io/cran/lawstat>.
- Pinheiro, J. 2009. nlme: Linear and nonlinear mixed effects models. Accessed June 27, 2017, at <https://cran.r-project.org/web/packages/nlme/index.html>.
- Lenth, R. V. 2016. Least-squares means: the R package lsmeans. *J. Stat. Softw.* **69**: 1–33.
- Aarts, E., M. Verhage, J. V. Veenliet, C. V. Dolan, and S. van der Sluis. 2014. A solution to dependency: using multilevel analysis to accommodate nested data. *Nat. Neurosci.* **17**: 491–496.

29. Mesaros, C., S. H. Lee, and I. A. Blair. 2009. Targeted quantitative analysis of eicosanoid lipids in biological samples using liquid chromatography-tandem mass spectrometry. *J. Chromatogr. B Analyt. Technol. Biomed. Life Sci.* **877**: 2736–2745.
30. Le Faouder, P., V. Baillif, I. Spreadbury, J-P. Motta, P. Rousset, G. Chêne, C. Guigné, F. Tercé, S. Vanner, N. Vergnolle, et al. 2013. LC-MS/MS method for rapid and concomitant quantification of pro-inflammatory and pro-resolving polyunsaturated fatty acid metabolites. *J. Chromatogr. B Analyt. Technol. Biomed. Life Sci.* **932**: 123–133.
31. Dasilva, G., M. Pazos, J. M. Gallardo, I. Rodríguez, R. Cela, and I. Medina. 2014. Lipidomic analysis of polyunsaturated fatty acids and their oxygenated metabolites in plasma by solid-phase extraction followed by LC-MS. *Anal. Bioanal. Chem.* **406**: 2827–2839.
32. Montuschi, P., G. Santini, S. Valente, C. Mondino, F. Macagno, P. Cattani, G. Zini, and N. Mores. 2014. Liquid chromatography-mass spectrometry measurement of leukotrienes in asthma and other respiratory diseases. *J. Chromatogr. B Analyt. Technol. Biomed. Life Sci.* **964**: 12–25.
33. Shaik, J. S. B., T. M. Miller, S. H. Graham, M. D. Manole, and S. M. Poloyac. 2014. Rapid and simultaneous quantitation of prostanoids by UPLC-MS/MS in rat brain. *J. Chromatogr. B Analyt. Technol. Biomed. Life Sci.* **945–946**: 207–216.
34. Szklenar, M., J. Kalkowski, V. Stangl, M. Lorenz, and R. Rühl. 2013. Eicosanoids and docosanoids in plasma and aorta of healthy and atherosclerotic rabbits. *J. Vasc. Res.* **50**: 372–382.
35. Bollinger, J. G., W. Thompson, Y. Lai, R. C. Oslund, T. S. Hallstrand, M. Sadilek, F. Turecek, and M. H. Gelb. 2010. Improved sensitivity mass spectrometric detection of eicosanoids by charge reversal derivatization. *Anal. Chem.* **82**: 6790–6796.
36. Varma, D., S. Ganti, T. Gilles, M. Diaz, T. Thompson, J. Stull, and S. A. Jansen. 2011. Comparison of UHPLC and HPLC methods for the assay of prostanoids: are the methods equivalent in terms of accuracy and precision? *Bioanalysis*. **3**: 853–862.
37. Prüss, H., B. Rosche, A. B. Sullivan, B. Brommer, O. Wengert, K. Gronert, and J. M. Schwab. 2013. Proresolutive lipid mediators in multiple sclerosis—differential, disease severity-dependent synthesis—a clinical pilot trial. *PLoS One*. **8**: e55859.
38. Chambers, E., D. M. Wagrowski-Diehl, Z. Lu, and J. R. Mazzeo. 2007. Systematic and comprehensive strategy for reducing matrix effects in LC/MS/MS analyses. *J. Chromatogr. B Analyt. Technol. Biomed. Life Sci.* **852**: 22–34.
39. Bodenlenz, M., B. Prietl, P. Florian, A. Subramaniam, S. Kainz, G. Rauter, T. R. Pieber, and F. Sinner. 2017. Characterization of the psoriasis-like inflammation in the imiquimod rat model using dermal open flow microperfusion. *J. Invest. Dermatol.* **137**: S278.
40. Birngruber, T., B. Prietl, M. Bodenlenz, P. Florian, A. Subramaniam, S. Kainz, G. Rauter, T. R. Pieber, and F. Sinner. 2016. Continuous sampling of immune cells using open flow microperfusion. *J. Invest. Dermatol.* **137**: S275.
41. Hammarström, S., M. Hamberg, E. A. Duell, M. A. Stawiski, T. F. Anderson, and J. J. Voorhees. 1977. Glucocorticoid in inflammatory proliferative skin disease reduces arachidonic and hydroxyeicosatetraenoic acids. *Science*. **197**: 994–996.
42. Fogh, K., T. Herlin, and K. Kragballe. 1989. Eicosanoids in skin of patients with atopic dermatitis: prostaglandin E2 and leukotriene B4 are present in biologically active concentrations. *J. Allergy Clin. Immunol.* **83**: 450–455.
43. Kendall, A. C., S. M. Pilkington, K. A. Massey, G. Sassano, L. E. Rhodes, and A. Nicolaou. 2015. Distribution of bioactive lipid mediators in human skin. *J. Invest. Dermatol.* **135**: 1510–1520.
44. Gilliet, M., C. Conrad, M. Geiges, A. Cozzio, W. Thürlimann, G. Burg, F. O. Nestle, and R. Dummer. 2004. Psoriasis triggered by toll-like receptor 7 agonist imiquimod in the presence of dermal plasmacytoid dendritic cell precursors. *Arch. Dermatol.* **140**: 1490–1495.
45. van der Fits, L., S. Mourits, J. S. Voerman, M. Kant, L. Boon, J. D. Laman, F. Cornelissen, A. M. Mus, E. Florencía, E. P. Prens, et al. 2009. Imiquimod-induced psoriasis-like skin inflammation in mice is mediated via the IL-23/IL-17 axis. *J. Immunol.* **182**: 5836–5845.
46. Flutter, B., and F. O. Nestle. 2013. TLRs to cytokines: mechanistic insights from the imiquimod mouse model of psoriasis. *Eur. J. Immunol.* **43**: 3138–3146.
47. Patel, U., N. M. Mark, B. C. Machler, and V. J. Levine. 2011. Imiquimod 5% cream induced psoriasis: a case report, summary of the literature and mechanism. *Br. J. Dermatol.* **164**: 670–672.
48. Yanaba, K., M. Kamata, N. Ishiura, S. Shibata, Y. Asano, Y. Tada, M. Sugaya, T. Kadono, T. F. Tedder, and S. Sato. 2013. Regulatory B cells suppress imiquimod-induced, psoriasis-like skin inflammation. *J. Leukoc. Biol.* **94**: 563–573.
49. Lin, Y., S. Yang, C. Chen, and H. Kao. 2015. Using imiquimod-induced psoriasis-like skin as a model to measure the skin penetration of anti-psoriatic drugs. *PLoS One*. **10**: e0137890.
50. Alvarez, P., and L. E. Jensen. 2016. Imiquimod treatment causes systemic disease in mice resembling generalized pustular psoriasis in an IL-1 and IL-36 dependent manner. *Mediators Inflamm.* **2016**: 6756138.
51. Chen, T., L. Fu, L. Zhang, B. Yin, P. Zhou, N. Cao, and Y. Lu. 2016. Paeoniflorin suppresses inflammatory response in imiquimod-induced psoriasis-like mice and peripheral blood mononuclear cells (PBMCs) from psoriasis patients. *Can J Physiol Pharmacol.* **94**: 888–894.
52. Luo, D., H. Wu, Y. Zhao, J. Liu, and F. Wang. 2016. Different imiquimod creams resulting in differential effects for imiquimod-induced psoriatic mouse models. *Exp. Biol. Med. (Maywood)*. **241**: 1733–1738.
53. Okazaki, S., S. Nagoya, H. Matsumoto, K. Mizuo, M. Sasaki, S. Watanabe, T. Yamashita, and H. Inoue. 2015. Development of non-traumatic osteonecrosis of the femoral head requires toll-like receptor 7 and 9 stimulations and is boosted by repression on nuclear factor kappa B in rats. *Lab. Invest.* **95**: 92–99.
54. Okasha, E. F., N. A. Bayomy, and E. Z. Abdelaziz. 2018. Effect of topical application of black seed oil on imiquimod-induced psoriasis-like lesions in the thin skin of adult male albino rats. *Anat. Rec. (Hoboken)*. **301**: 166–174.
55. Baer, A. N., P. B. Costello, and F. A. Green. 1990. Free and esterified 13(R,S)-hydroxyoctadecadienoic acids: principal oxygenase products in psoriatic skin scales. *J. Lipid Res.* **31**: 125–130.
56. Bodenlenz, M., C. Höfferer, C. Magnes, R. Schaller-Ammann, L. Schaupp, F. Feichtner, M. Ratzner, K. Pickl, F. Sinner, A. Wutte, et al. 2012. Dermal PK/PD of a lipophilic topical drug in psoriatic patients by continuous intradermal membrane-free sampling. *Eur. J. Pharm. Biopharm.* **81**: 635–641.